CGMS-XXXI EUM-WP-19
Prepared by EUMETSAT
Agenda Item: II/4

# DERIVING GLOBAL SURFACE ALBEDO MAPS FROM GEOSTATIONARY WEATHER SATELLITES

Monitoring and understanding climate changes of the Earth require the generation of long-term and consistent and global data set from observation. In this context, geostationary satellite observations could play a significant role thanks to the long duration of the missions and the corresponding archives. In particular, the frequent cycle of acquisition can be used to document the anisotropy of the surface and therefore surface albedo. This paper discusses thus the possibility to generate a global surface albedo map from the different geostationary satellites, accounting for the technical differences between their respective instrument. As a pilot study, the product consistency between two adjacent spacecrafts (Meteosat-5 and -7) is evaluated with an analysis of the common observed area.

# Deriving Global Surface Albedo Maps from Geostationary Weather Satellites

*Y.M. Govaerts*[1], *A. Lattanzio*[1], *B. Pinty*[2] *and J. Schmetz*[1]

(1) EUMETSAT, Postfach 10 05 55, D-64295 Darmstadt, Germany
(2) IES/JRC/CEC, I-21020 Ispra, Italy

## 1 Introduction

Observations from operational meteorological satellites, composed both of polar-orbiting and geostationary platforms, play an increasing role in documenting climate variations thanks to the duration of their respective archive, often covering three decades or more (Ohring and Gruber 2001). During the late seventies and early eighties, space-borne observations of the Earth were very scarce, essentially limited to geostationary meteorological observations and a few polar platforms. The instruments onboard these satellites as well as their routine operation procedures were however not originally conceived to support such objectives. Consequently, a number of basic issues like uncontrolled orbit drift, geo-rectification accuracy or poorly calibrated and characterized sensors need to be addressed first. Nevertheless, observations acquired by these instruments have already proven to be useful in a number of areas such as atmospheric temperature (*e.g.*, Christy et al. 2000), sea surface temperature (*e.g.*, Strong et al. 2000), or cloud cover (Rossow et al. 1985). As concerns land surface characterization, snow cover (*e.g.*, Robinson 2000), vegetation indices (*e.g.*, Myneni et al. 1997) and the Fraction of Absorbed Photosynthetically Active Radiation (FAPAR) or surface albedo (*e.g.*, Ba et al. 2001) are typical parameters that have been derived from meteorological satellites.

Among these parameters, the albedo of the Earth's surface is a critical variable for climate studies, as it controls the fraction of solar energy available to the surface (*e.g.*, Dickinson 1983)). Although the potential of space-based observations to retrieve globally this parameter has long been recognized, it is only routinely derived since 2001 from the Moderate- Resolution Imaging Spectroradiometer (MODIS) and Terra/Multiangle Imaging SpectroRadiometer (MISR) instruments onboard the Terra platform (Jin et al. 2003, Martonchik et al. 1998). Unfortunately, the systematic generation of surface albedo from archived observation from meteorological platforms has only received limited attention so far. Consequently, long-term surface albedo - atmosphere feedback mechanisms as predicted by Charney (1975) are still poorly quantified. This situation results in part from the lack of adequate data to properly solve the radiative transfer problem. Actually, the solution of this problem requires to account both for the effects of the aerosol-loaded atmosphere and to document surface reflectance at different illumination and viewing angles. This latter information is not directly available from traditional mono-directional space observations. Except for instruments specifically designed to acquire almost simultaneously multi-angular observations, a temporal accumulation is necessary to collect reflectance acquired with different viewing angles. The duration of such accumulation period can exceed two weeks on polar platform, a period during which surface radiative properties are assumed to be stable.

In this context, the capacity of geostationary satellites to acquire data at a relatively high temporal frequency opens new opportunities to document these angular effects, at least for those places and time periods for which the surface-atmosphere system does not change too fast over a day. Assuming that the reciprocity principle can be applied over land surfaces at a spatial resolution of few kilometers, a data accumulation period limited to the course of the day provides a rather good sampling in the directional domain, since the illumination geometry will change continuously and predictably during such a period. Hence, in addition to traditional spectral observations, geostationary satellites bring a useful angular information thanks to their frequent acquisition time. The possibility to exploit this principle for the generation consistent surface albedo maps from Meteosat VIS

band observations has recently been demonstrated by Pinty et al. (2000a).

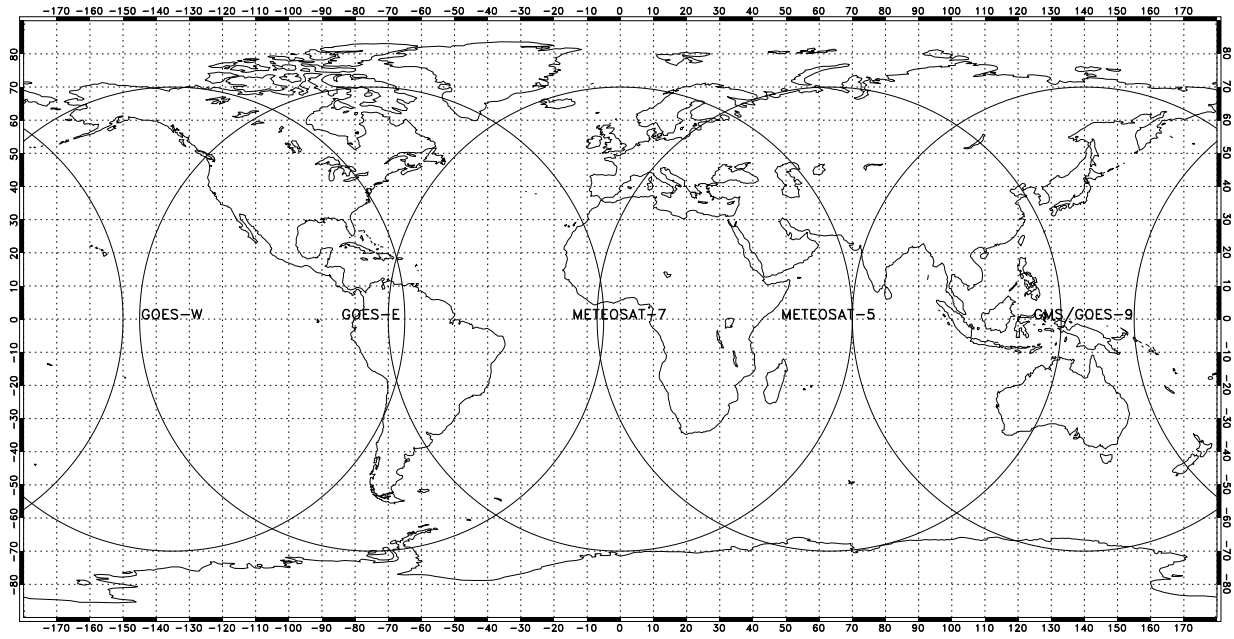


Figure 1: Location of the current operational geostationary satellites with systematic archived data. Circles show the 70° viewing angle limit.

A global view of the Earth from the geostationary orbit, with the exception of the poles, is ensured by a suite of operational meteorological satellites located at regular interval along the Equator (Fig. 1). All radiometers onboard these instruments observed the Earth with a broad solar channel ranging approximately from 0.6 up to 0.8$\mu$m, referred to as the VIS band. In principle, the algorithm proposed by Pinty et al. (2000a) could be applied to any of these geostationary satellites, whatever their sub-satellite position along the Equator. Additionally, the overlapping region between two adjacent spacecrafts could be advantageously used to evaluate the consistency of these products derived from two different viewing geometries. Recently, the Global Climate Observing System (GCOS) committee recognized the need for establishing a benchmark for assessing land-surface albedo product and implementing a system for the retrieval of surface albedo from existing and archived geostationary satellites to form a global climatology of albedo for the entire period of available measurements (GCOS 2003). An early proof of this concept, based on the data processing of two European geostationary satellites currently operated by EUMETSAT at 0 and 63° East, is presented in this paper.

## 2 Surface albedo retrieval from geostationary satellites

Surface albedo should be estimated by integrating the bidirectional spectral reflectance of the surface over all angles of the upward hemisphere. Retrieving surface albedo from space observations requires thus to account for scattering and absorption processes in the atmosphere, and to document the angular anisotropy of the surface, accounting for the radiative coupling between both systems. The accuracy achieved in the albedo estimation depends on the density of the angular sampling and the reliability of the atmospheric correction. Since the anisotropy of natural surfaces is highly variable in space and time, sufficient sampling of the bidirectional reflectance fields is therefore crucial. Additionally, it is difficult to accurately characterize the surface without simultaneously quantifying the interactions of the radiation field with the atmosphere because the surface constitutes one of the boundary conditions of the radiation transfer problem that needs to be solved when analyzing remote sensing data. Surface albedo retrieval approaches should thus treat the surface and atmosphere as a coupled radiative system.

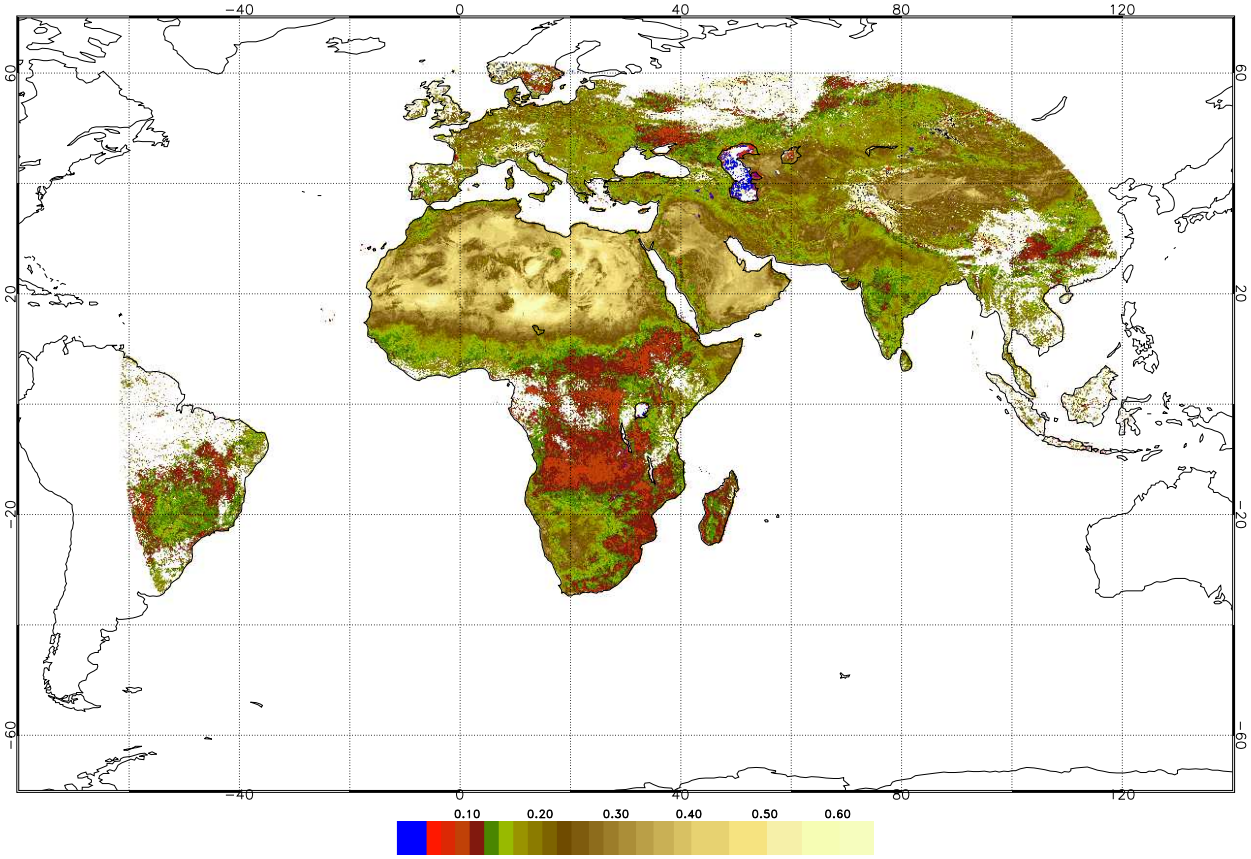


Figure 2: MSA map derived with Meteosat-5 and -7 for a 10 day composite period running from May 1–10 1999.

This task is not trivial as scattering processes in an aerosol-loaded atmosphere and at the surface (*i.e.*, soil and vegetation) are quite different. Numerous approaches have been proposed in the past to derive surface albedo from geostationary observations, (*e.g.*, Pinty and Ramond 1987, Nacke 1991, Pinker and Laszlo 1992), most of them ignoring the surface anisotropy or imposing atmospheric conditions. Recently, Pinty et al. (2000a) revisited these techniques and proposed a new method to characterize simultaneously surface anisotropy and atmospheric scattering properties, explicitly accounting for the radiative coupling between these two systems. The approach relies on a daily accumulation of Meteosat daylight observations acquired at about 20 different illumination conditions to characterize the scattering properties of the surface and the atmosphere, assuming that i) surface and atmospheric scattering properties are constant along the day, ii) continental aerosol type applied everywhere and all year long, iii) surface anisotropy can be represented with the simple Bidirectional Reflectance Factor (BRF) model proposed by Rahman et al. (1993) and finally iv) the reciprocity principle is valid over terrestrial surfaces at a spatial resolution of a few kilometers. The Meteosat Surface Albedo (MSA) algorithm has been implemented in the EUMETSAT ground segment where the VIS band calibration is performed routinely with an advanced algorithm relying on simulated spectral radiances. The accuracy of these simulated radiances has been verified against well calibrated instruments and are a close to 3% (Govaerts and Clerici 2003). Directional Hemispherical Reflectance (DHR30) values corrected for atmospheric effects are derived for every processed day for a Sun zenith angle fixed at 30°. A simple composite procedure is applied over consecutive 10-days period to produce geographically complete maps of surface albedo (Pinty et al. 2000b). This product is generated at the Meteosat full spatial resolution which corresponds to a North-South and East-West sampling distance of about 2.5 km at the sub-satellite point (Table 1). Additionally, as solar radiation is taking its maximum in the Meteosat radiometer VIS band spectral interval, the MSA is almost linearly related to broadband albedo.

Table 1: Characteristics of the archived data from various geostationary instruments shown on Fig. (1).

| Location | Period[(a)] | Satellite | Sensor | VIS band[(b)] | Rep. cycle[(c)] | S. Dist.[(d)] | Digit. |
|---|---|---|---|---|---|---|---|
| 0° | 1981 – 1989 | Meteosat-1,2,3 | MVIRI | 0.4 – 1.1 | 30/60 min | 2.5 km | 6 bits |
| | 1989 – now | Meteosat-4,5,6,7 | MVIRI | 0.4 – 1.1 | 30 min | 2.5 km | 8 bits |
| 63°E | 1998 – now | Meteosat-5 | MVIRI | 0.4 – 1.1 | 30 min | 2.5 km | 8 bits |
| 140°E | 1987 – 2003 | GMS-3,4,5 | VISSR | 0.55 – 0.80 | 60 min | 1.25 km | 6bits |
| 135°W | 1981 – 1989 | GOES-4,6[(e)] | VISSR | 0.55 – 0.75 | 30 min | 0.9km | 6bits |
| | 1996 – now | GOES-9,12[(e)] | | 0.55 – 0.75 | 60 min | 1 km | 10bits |
| 75°W | 1981 – 1997 | GOES-5,7[(e)] | VISSR | 0.55 – 0.75 | 30 min | 0.9km | bits |
| | 1997 – now | GOES-8,10[(e)] | | 0.55 – 0.75 | 60 min | 1 km | bits |

(a) When data are available from the archive.
(b) Approximate spectral range in $\mu$m.
(c) Average repeat cycle available from the archive.
(d) Sampling distance at the sub-satellite point.
(e) The satellite has been moved during the operational mission.

# 3 Towards a global mapping

Such algorithm is not limited to a specific satellite position and could be in principle applied to any calibrated geostationary observations in the solar region, provided the temporal sampling is high enough. Since July 1998, EUMETSAT is operating simultaneously two geostationary Meteosat spacecrafts, one located at 0 degree longitude (Meteosat-7) and one located at 63 ° East (Meteosat-5), originally in support to the INDian Ocean EXperiment (INDOEX). The MSA algorithm has been used to retrieve surface albedo over the 0° and 63°E missions. Albedo values generated from both spacecrafts have been re-mapped on a common grid (Fig. 2) and cover most of Europe, Africa and large part of Asia up to about 60° North. Since the two observation areas largely overlap as can be seen on Fig. (1), comparison of albedo values in this common region offers a unique opportunity to evaluate the consistency of a same product retrieved from two instruments located at two different places.

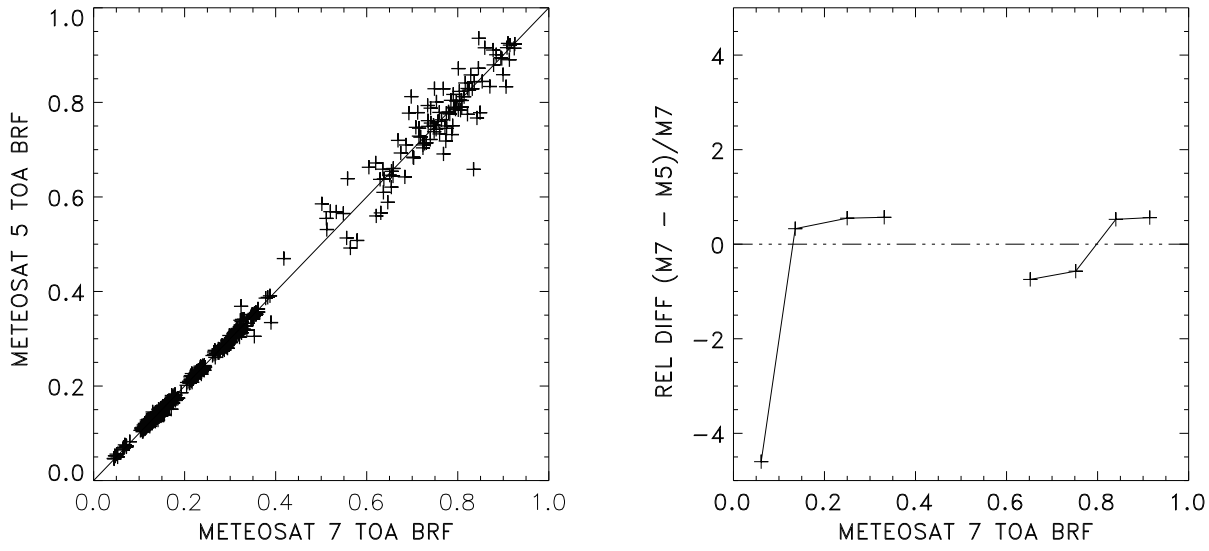


Figure 3: **LEFT**: TOA BRF scatter plot derived from Meteosat -7 and -5 along the 31.5°W longitudinal transect. **RIGHT**: Relative difference in percent between the Meteosat-7 and -5 TOA BRF as a function of the Meteosat-7 TOA BRF.

The inter-calibration consistency between the two instruments is evaluated first. This step is critical prior

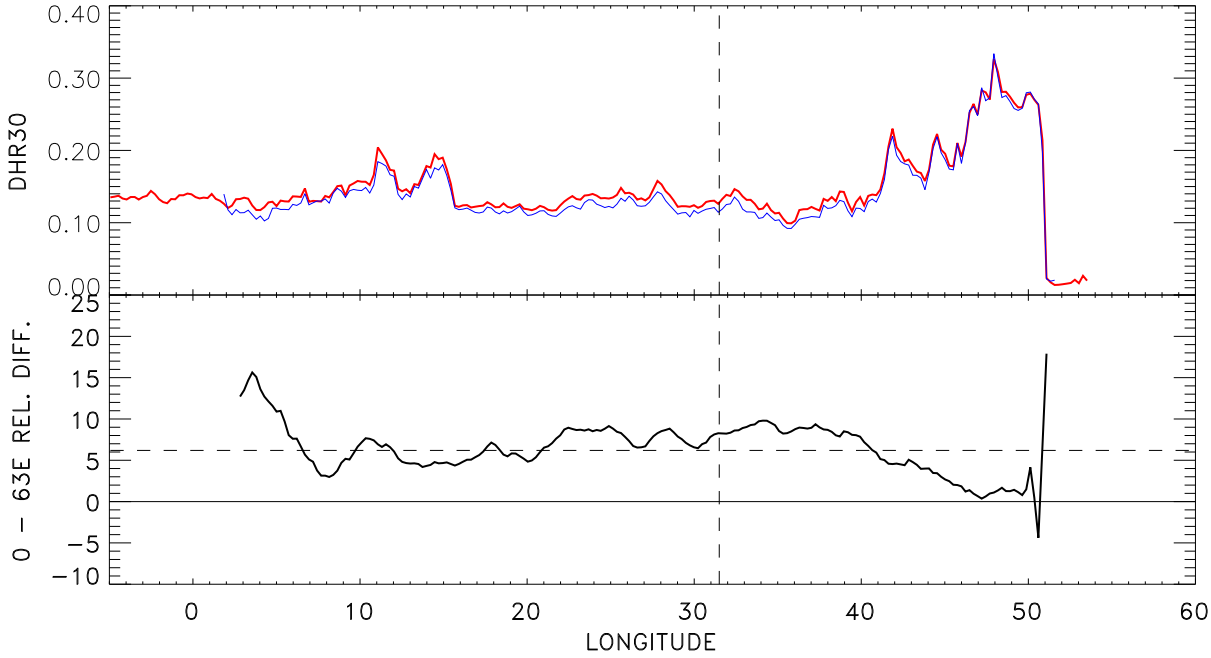


Figure 4: **TOP**: DHR30 profile along a latitudinal transect located at a 10° North derived from Meteosat-5 (blue) and Meteosat-7 (red). **BOTTOM**: Relative difference in percent between DHR30 values derived from Meteosat-7 (0°) and Meteosat-5 (63°). The horizontal dashed line shows the men relative difference.

to any product comparison as uncertainties in the characterization of spectral response of the Meteosat-5 instrument VIS band have already been reported (Govaerts 1999). Top-of-Atmosphere (TOA) BRF derived for both instruments under similar viewing and sun zenith angles, *i.e.*, when the relative azimuth angles is close to zero or 180° have been collected. There is a very good agreement between both instruments as can be seen in Fig. 3, left plot. A detailed analysis of the relative difference between both signals, shown on the right panel, reveals however some discrepancy, in particular over dark sea surfaces, where the TOA BRF is close to 0.05 in the Meteosat VIS band. Such result might indicate some minor linearity problem with one of the instrument as a 5% difference corresponds to about half a digital count value over sea surfaces. The sharp transition between sea and terrestrial surfaces, where the TOA BRF typically ranges from 0.1 to 0.4, rather suggests a possible Meteosat-5 spectral response error around 0.4$\mu$m, where spectral radiance over sea takes its maximum value. Over terrestrial surfaces, observations are very consistent, Meteosat-7 reflectances overestimating only by less than 1% those observed by Meteosat-5.

The retrieved DHR30 values are analyzed next. To this end, four different periods of 1999 corresponding to Julian days 31–40, 121-130, 211-220 and 301-310 have been compared. On the average, DHR30 values retrieved from Meteosat-7 observations over the common area exceed by about 5.5% those retrieved from Meteosat-5. Several factors might explain this difference. First, as already mentioned, inaccuracies in the spectral response might be responsible for some systematic errors. Sensitivity analysis shows that spectral response uncertainties translates in radiance simulation error of about 3 to 6% for Meteosat-7 and 15% for Meteosat-5, depending on the surface type. As these uncertainties essentially affect short wavelength regions (Kriebel et al. 1996), they might systematically impact the estimation of the aerosol load. Systematically different illumination conditions between the two spacecraft in the common areas need also to be considered. In that region, pixels observed by Meteosat-5 (63° East) correspond more often to back scattering conditions whereas forward scattering conditions dominate Meteosat-7 observations. The impact of these differences is analyzed in detailed along a latitudinal transect extracted at 10°N. DHR30 profiles derived from both instruments, averaged for the four selected periods is shown on Fig. (4). Along such transect, the viewing zenith angles is similar for the two

instruments only at 31.5°E. The relative difference between the two profiles is not constant, but does not exhibit clear trends as a function of the longitude, *i.e.*, the viewing angle. Conversely, the relative difference shows a trend as a function of the DHR30 magnitude, ranging from differences close to zero when surface albedo takes large values up to 5–10% over dark surfaces. Additional in-depth analysis of these difference would clearly be needed but are beyond the scope of this proof-of-concept paper. It has however demonstrated the impact of uncertainties in the characterization of the radiometer actual performance on the product accuracy.

# 4 Discussion and conclusion

Geostationary satellite observations acquired at a high temporal resolution of one hour or less open new avenue to document scattering processes in the aerosol-loaded atmosphere and at the surface. Although these observations are limited to one single wide VIS band, the daily angular sampling permits to derive consistent albedo maps. An analysis of the Meteosat-5 and -7 overlapping area shows that these products agree within a relative error of about 6%. This error is largely attributed to uncertainty in the actual instrument characteristics, stressing the need for space agencies to increase their archived data stewardship through reprocessing and recalibration efforts. Once clearly understood and defined, such uncertainties could be introduced in the retrieval algorithm to increase the usefulness of the generated product by including credible error estimations.

The generation of a global albedo climatology, as recommended by GCOS (2003) requires an in-depth analysis of the actual status of the archived geostationary satellite data, as the characteristics of these instruments have evolved in time and differ from agency to agency (Table 1). The challenges and problems related to different spectral, temporal or spatial resolution will have to be carefully addressed. Such a surface albedo climatology derived from meteorological geostationary satellites could usefully complement land surface products on the vegetation status derived for the last two decades from mono-angular multi-spectral sensors on meteorological polar-orbiting platforms.

# References


Ba, M. B., R. Frouin, S. E. Nicholson, and G. Dedieu (2001). Satellite-derived surface radiation budget over the African continent. Part I: estimation of downawrd solar irradiance and albedo. *J. Climate 14*, 45–58.

Charney, J. G. (1975). Dynamics of deserts and droughts in the Sahel. *Quaterly Journal of the Royal Meteorological Society 101*, 193–202.

Christy, J. R., R. W. Spencer, and W. D. Braswell (2000). MSU Tropospheric temperatures: Data set construction and radiosonde comparisons. *Journal of Atmospheric and Oceanic Technology 17*, 1153–1170.

Dickinson, R. E. (1983). Land surface processes and climate-surface albedos, Adv. Geophys., 25, 305353, 1983. *Adv. Geophys. 25*, 305–353.

GCOS (2003). Second report on the adequacy of the global observing systems for climate. Technical Report GCOS-82 (WMO/TD No 1143), World Meteorological Organization, pp 74.

Govaerts, Y. M. (1999). Correction of the Meteosat-5 and -6 VIS band relative spectral response with Meteosat-7 characteristics. *International Journal of Remote Sens. 20*, 3677–3682.

Govaerts, Y. M. and M. Clerici (2003). Evaluation of Radiative Transfer Simulations over Bright Desert Calibration Sites. *IEEE Transactions on Geoscience and remote sensing in print*.

Jin, Y., C. B. Schaaf, F. Gao, X. Li, A. H. Strahler, W. Lucht, and S. Liang (2003). Consistency of MODIS surface bidirectional reflectance distribution function and albedo retrievals: 1. Algorithm performance. *Journal of Geophysical Research 108*, 4158, doi:10.1029/2002JD002803.

Kriebel, K. T., H. Mannstein, and V. Amann (1996). Absolute calibration of the Meteosat-5 visble channels. In EUMETSAT (Ed.), *1996 Meteorological Satellite Data Users' Conference*, Vienna, pp. 31–40.

Martonchik, J. V., D. J. Diner, B. Pinty, M. M. Verstraete, R. B. Myneni, Y. Knyazikhin, and H. R. Gordon (1998). Determination of land and ocean reflective, radiative, and biophysical properties using multiangle imaging. *IEEE Transaction on Geosciences and Remote Sensing 36*, 12661281.

Myneni, R. B., C. D. Keeling, C. J. Tucker, G. Asrar, and R. R. Nemani (1997). Increased plant growth in the northern high latitudes from 1981 to 1991. *Nature 386*, 698–702.

Nacke, G. (1991). Surface albedo derived from Meteosat imagery with application to Africa. *Journal of geophysical Research 96*, 18581–18601.

Ohring, G. and A. Gruber (2001). Climate monitoring from operational satellites: accomplishments, problems, and prospects. *Advance in Space Research 28*, 207–219.

Pinker, R. T. and I. Laszlo (1992). Modeling surface solar irradiance for satellite applications on a global scale. *Journal of Applied Meteorology 31*, 194–211.

Pinty, B. and D. Ramond (1987). A method for estimate of broadband directional surface albedo from a geostationary satellite. *Journal of Climate and Applied Meteorology 26*, 1709–1722.

Pinty, B., F. Roveda, M. M. Verstraete, N. Gobron, Y. Govaerts, J. V. Martonchik, D. J. Diner, and R. A. Kahn (2000a). Surface albedo retrieval from Meteosat: Part 1: Theory. *Journal of Geophysical Research 105*, 18099–18112.

Pinty, B., F. Roveda, M. M. Verstraete, N. Gobron, Y. Govaerts, J. V. Martonchik, D. J. Diner, and R. A. Kahn (2000b). Surface albedo retrieval from Meteosat: Part 2: Applications. *Journal of Geophysical Research 105*, 18113–18134.

Rahman, H., B. Pinty, and M. M. Verstraete (1993). Coupled surface-atmosphere reflectance (CSAR) model. 2. Semiempirical surface model usable with NOAA Advanced Very High Resolution Radiometer Data. *Journal of Geophysical Research 98*, 20,791–20,801.

Robinson, D. A. (2000). Weekly Northern Hemisphere Snow Maps: 1966-1999. In AMS (Ed.), *12th Conference on Applied Climatology*, Asheville, NC, pp. 12–15.

Rossow, W. B., F. Mosher, E. Kinsella, A. Arking, M. Desbois, E. Harrison, P. Minnis, E. Ruprecht, G. Seze, C. Simmer, and E. Smith (1985). ISCCP cloud algorithm intercomparison. *Journal of Climate and Applied Meteorology 24*, 877–903.

Strong, A. E., E. J. Kearns, and K. K. Gjovig (2000). Sea Surface Temperature Signals from Satellites - An Update. *Geophysical Research Letters 27*, 1667 – 1670.